PCCP

Accepted Manuscript

ROYAL SOCIETY OF CHEMISTRY

www.rsc.org/pccp

Chemical Communications

RSCPublishing

COMMUNICATION

Relating structure and photoelectrochemical properties: electron injection by structurally and theoretically characterized transition metal-doped phenanthroline-polyoxotitanate nanoparticles

Cite this: DOI: 10.1039/xoxxoooooox

Received ooth January 2012,
Accepted ooth January 2012

DOI: 10.1039/xoxxoooooox

www.rsc.org/

Katarzyna N. Jarzembska,[a,b] Yang Chen,[a] Justin N. Nasca,[a] Elżbieta Trzop,[a] David F. Watson[a] and Philip Coppens[a]

Whereas a large number of sensitized polyoxotitanate clusters have been reported, information on the electrochemical properties of the fully structurally defined nanoparticles is not available. Bridging of this gap will allow a systematic analysis of the relation between sensitizer-cluster binding geometry, electronic structure and electron injection properties. $Ti_{17}O_{28}(O^iPr)_{16}(Fe^{II}Phen)_2$ is a member of a doubly-doped series of nanoclusters in which the phenanthroline is attached to the surface-located transition metal atom. The visible spectrum of a dichloromethane solution of the studied sample shows a series of absorption bands in the 400-900 nm region. Theoretical DOS and TDDFT calculations indicate that the bands in increasing wavelength order correspond essentially to metal-to-core charge transfer (MCCT) at ~ 460 nm, metal-to-ligand charge transfer (MLCT) at ~ 520 nm and *d-d* metal-atom transitions. Exposure of a thin layer of the sample to light in a photoelectrochemical cell produces an electric current in the 400 − ~640 nm region. The fit of the wavelength range of the electron injection with the results of the calculations suggests that charge injection into the FTO anode occurs both from the TiO cluster and from the phenanthroline ligand. Injection from the phenanthroline via the cluster orbitals is ruled out by the lower energy of the phenanthroline orbitals.

Functionalized polyoxotitanate particles have been extensively employed as models for photo-induced electron injection in photoelectrochemical cells. Electron injection by $Fe(CN)_6^{4-}$absorbed on the surface of TiO_2 was first studied by Vrachnou *et al.,* who measured a large quantum yield on exposure of the orange-colored complex with visible light.[1] The kinetics of the back-electron transfer (ET) reaction were measured by Lu *et al*, and reported to include a relatively short exponential decay with τ = 270 ns, plus a μs-ms timescale non-exponential decay.[2] In agreement with the slow timescale for recombination, Lian and co-workers conclude from ultrafast IR and visible measurements of the back ET, and from the earlier measurements that the back ET process is highly non-exponential with time constants ranging from 3 ps to 3 μs.[3] However, notwithstanding the extensive evidence, direct measurements of the photocurrent generated by a fully structurally-defined sensitized cluster are extremely rare. A first report was published by Wu *et al.*[4] who synthesized two metal-phenanthroline fused Ti_{17} clusters, $Ti_{17}O_{28}(O^iPr)_{16}(Co^{II}Phen)_2$ and $Ti_{17}O_{28}(O^iPr)_{18}(Cd^{II}Phen)_2$, and subsequently found that a 2 − 2.5 μm film of the Co derivative deposited on an indium-tin oxide (ITO) electrode, inserted in a aqueous Na_2SO_4 electrolyte, produced a photocurrent described as cathodic of about 4 μA when exposed to repetitive 20 s light pulses from a Xenon lamp. However, the nature of the exposed film employed in this experiment is somewhat uncertain, as the moisture sensitive samples were prepared under ambient atmosphere, with a humidity of ~50%, the electrolyte used was aqueous, and the Raman spectrum of the film differs considerably from that of the polyoxotitanate cluster, while the wavelength dependence of the injection was not established.

To further examine the electron injection properties of this interesting system, we have synthesized several analogs with different transition metals. The most interesting in terms of electron injection properties is the iron analogue, $Ti_{17}O_{28}(O^iPr)_{16}(Fe^{II}Phen)_2$. We report here the structure of the brown-orange crystals, and the wavelength dependence of the photocurrent, which is found to be anodic, measured on a thin film in a Grätzel-type photoelectrochemical cell. The photo-induced current is transition-metal specific. It is significantly weaker for the Co-containing complex and fully absent in the visible region for both the Mn analogue and for the unsubstituted $Ti_{17}O_{24}(O^iPr)_{20}$ reference sample.

$Ti_{17}O_{28}(O^iPr)_{16}(Fe^{II}Phen)_2$ was prepared by solvothermal synthesis in a sealed pyrex tube of an anhydrous propanol solution of $Ti(O^iPr)_4$ (0.2 ml, 0.67 mmol), $Fe(OAc)_2$ (11.7 mg, 0.067 mmol) and 1,10-phenanthroline monohydrate (13.3 mg, 0.067 mmol). The mixture was heated to 150°C for 4 days and then cooled to 40°C and left for the next 3 days. During an additional week at room temperature, small brownish-orange block crystals were obtained. X-ray data were collected at 90 K on a Bruker AXS Kappa APEX II Ultra diffractometer equipped with a TXS rotating anode (Mo-K_α

radiation, λ = 0.71073 Å) and Helios optics. Its structure is fully described in the CIF file (CCDC 977543). The cluster (Fig. 1) consists of a Ti_{17} core, as described earlier,[5,6] functionalized with two attached Fe-phenanthroline groups, with a pseudo-octahedral coordination of the Fe atoms. The coordination geometry of the metal atom corresponds to a high-spin Fe^{II} configuration. The absorption spectrum of the complex in a dichloromethane solution, shown in Fig. 2, is similar to that of the solid-state sample of the Co analogue, reported by Wu *et al*,[4] and to that reported by Vrachnou *et al*,[1] who both assigned the bands at about at 350 − 600 nm as charge transfer (CT) band. This assignment is supported by our theoretical calculation discussed below.

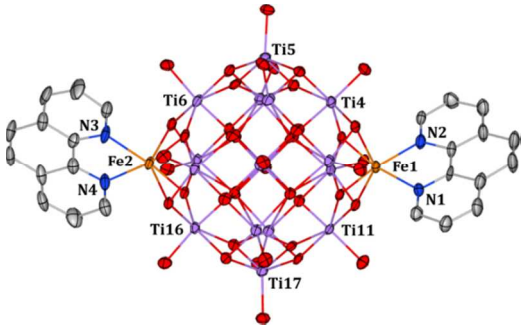

Figure 1. Molecular structure of the $Ti_{17}O_{28}(O^iPr)_{16}(Fe^{II}Phen)_2$ nanocluster (hydrogen atoms and ^{i}Pr groups are omitted for clarity; 50% probability ellipsoids).

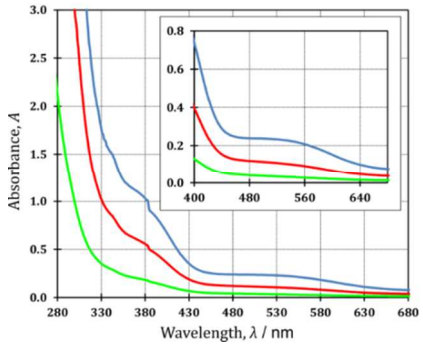

Figure 2. UV-Vis spectra of a $Ti_{17}O_{28}(O^iPr)_{16}(Fe^{II}Phen)_2$ solution in dichloromethane at concentrations of 0.2 mM (blue solid line), 0.1 mM (red solid line), and 0.025 mM (green solid line). The 400 – 680 nm region is magnified in the insert. The absorption spectrum of a single crystal in the 450-650 nm range is shown in the Supporting Information (Figure 4S).

Photoelectrochemical measurements were performed in a Teflon cell with a fluorine doped tin oxide (FTO) electrode covered with crystalline $Ti_{17}O_{28}(O^iPr)_{16}(Fe^{II}Phen)_2$ and a Pt counter electrode. The equipment has been described elsewhere.[7,8] The identity of the sample was confirmed by powder diffraction. An acetonitrile solution of $I_3^-I^-$ was used for the redox shuttle. The film was exposed with monochromatized light from a 75 W Xenon source. Details can be found in the Supporting Information.

The generated photocurrent is plotted against the exciting wavelength in Fig. 3 for three successive experiments on samples of increasing thickness. As shown, an anodic photocurrent is observed in the 400 − 640 nm region, but tapers off strongly beyond ~520 nm. The corresponding IPCE (Incident Photon to Current Efficiency) is presented in Figure 1S in the Supporting Information. Although the current is weak compared to that in electrochemical cells optimized for efficiency,[9] the results are fully reproducible. The lower intensity is tentatively attributed to the alkoxide shell enveloping the oxotitanate core, which reduces the contact with the FTO electrode and hampers charge flow between the nanoparticles and between the nanoparticles and the electrolyte, as occurs in microporous anatase used in cells optimized for electricity production.[9] It may be noted the observed photocurrent decreases with increasing thickness of the $Ti_{17}O_{28}(O^iPr)_{16}(Fe^{II}Phen)_2$ layer, indicating that charge flow is reduced with increasing thickness of the layer. No photocurrent is observed when a sample of the parent Ti_{17} cluster is examined in the same cell, as shown by the black curves in Fig. 3.

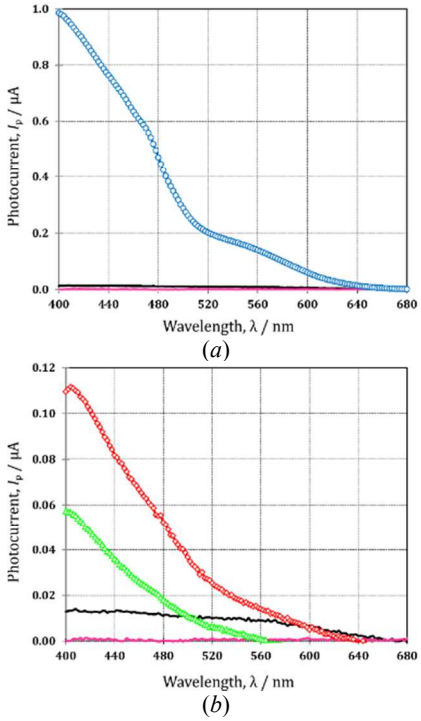

Figure 3. (*a,b*) Photocurrent measured with the $Ti_{17}O_{28}(O^iPr)_{16}(Fe^{II}Phen)_2$ nanocluster films on FTO glass in three successive experiments with samples of increasing thickness in the 10 – 100 μm range (in order of increasing thickness: blue circles, red rhombs, green triangles). The black and pink lines represent respectively the results of reference experiments conducted with a Ti_{17} covered FTO electrode and a plain FTO slide as working electrode.

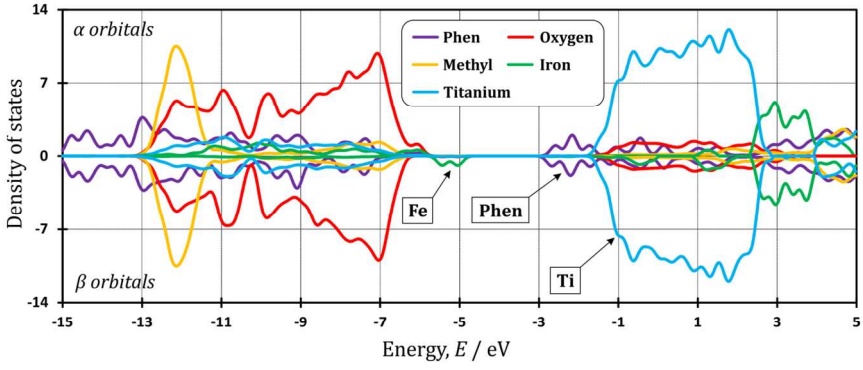

Figure 4. $Ti_{17}O_{28}(O^iPr)_{16}(Fe^{II}Phen)_2$ DOS calculated at the PBE0/LANL2DZ level of theory.

Theoretical calculations were performed to identify the absorption in the photoactive region. Results obtained with the PBE0/LANLDZ method show two Fe-β orbitals located within the band gap, as illustrated in the partial density of states (DOS) shown in Fig. 4. The corresponding diagram for the Ti_{17} cluster is shown in Fig. 2S. Time-dependent density functional theory (TDDFT) calculations were carried out to explore the nature of the excitations corresponding to the observed absorption bands. The calculated spectrum is shown in Fig. 5. It has similar features as the observed solution spectrum (Fig. 2), although the theoretical results are somewhat shifted relative to the observations, a discrepancy attributed to approximations in the calculations. The calculations show MLCT transitions from the closely spaced (by 0.4 eV) pseudo-symmetry related β-HOMO-1 and β-HOMO Fe *d*-orbitals, which are the orbitals located at the lower edge of the band gap in the DOS diagram (Fig. 4), to the phenanthroline ligands. Some of the more intense transitions to the phenanthroline occur at 519 nm and 508 nm with oscillator strengths (f) of 0.0094 and 0.0110, respectively. As expected, pseudo-symmetry related transitions occur at the other half of the molecule. As the MLCT absorption leads to a component of the electron injection into the FTO anode, and the phenanthroline energy levels are below those of the cluster, this suggests direct injection from the phenanthroline ligands, which are not covered by alkoxide groups, into the FTO anode.

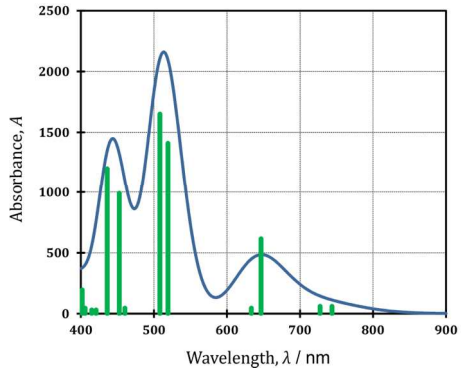

Figure 5. The calculated visible range of the electronic spectrum of $Ti_{17}O_{28}(O^{i}Pr)_{16}(Fe^{II}Phen)_2$ at the PBE0/LANL2DZ level of theory; green lines denote relative oscillator strengths. The three bands correspond to MCCT (~450 nm), MLCT (~510 nm), mixed transitions from Fe orbitals (~650 nm) and Fe *d*-*d* transitions (~725 nm).

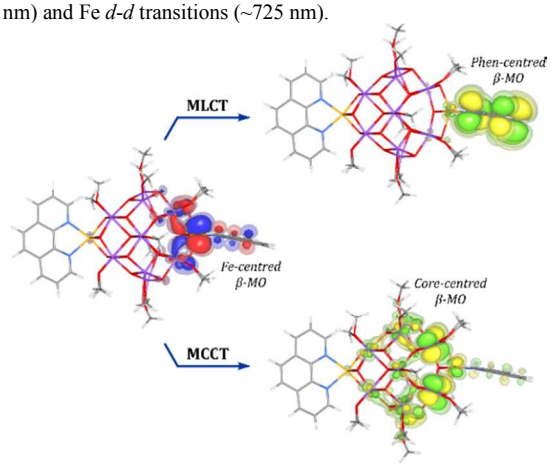

Figure 6. Top: MLCT, metal-to-ligand charge transfer from the Fe to the phenanthroline ligand involving β molecular orbitals, HOMO-1 and LUMO+2 (519 nm). Bottom: MCCT, metal-to-core charge transfer, the electron injection into the polyoxotitanate-core from the β-HOMO-1 to orbital β-LUMO+4 (466 nm). Isovalues at 0.02 a.u. (solid surfaces) and 0.01 a.u. (semi-transparent surfaces). (Note: for clarity structure rotated by ~45° around a horizontal axis relative to the one depicted in Fig. 1.)

Electron transfer from the metal into the polyoxotitanate core is found mainly, but not exclusively, from the HOMO-1 and HOMO levels at wavelengths of 436 nm (f = 0.0080) and 453 nm (f = 0.0066), which is in good agreement with the observed spectroscopic data and previous assignments for $Fe(CN)_6^{4-}$ sensitized TiO_2.[1] Two transitions from the HOMO-1 level at 519 nm and 436 nm are shown in Fig. 6.

We conclude that the work points the way to establishing the relation between the photoelectrochemical properties and the detailed structure of sensitized nanoparticles. In addition, the combination of a well-defined crystalline sample of known structure with characterization of the electron injection induced by light in the visible range opens the possibility of synchrotron time-resolved diffraction studies[10,11] of the geometric change on injection and recombination.

Research supported by the Office of Basic Energy Sciences of the U.S. Department of Energy through grant DE-FG02-02ER15372. KNJ thanks the Polish Ministry of Science and Higher Education for financial support within the "Mobility Plus" program and the Foundation for Polish Science for financial support within the "START" program.

Notes and references

[a] *Department of Chemistry, University at Buffalo, The State University of New York, Buffalo, NY 14260-3000, USA. E-mails: coppens@buffalo.edu, dwatson3@buffalo.edu.*
[b] *Department of Chemistry, University of Warsaw, Pasteura 1, 02-093 Warszawa, Poland.*

† Electronic Supplementary Information (ESI) available: Details on the synthesis, crystallography, electrochemical measurements and theoretical calculations. See DOI: 10.1039/c000000x/. The CIF file with detailed crystallographic information is available freely from the Cambridge Structural Database (deposition number: CCDC 977543).

1. E. Vrachnou, N. Vlachopoulos and M. Gratzel, *Journal of the Chemical Society-Chemical Communications*, 1987, 868.
2. H. Lu, J. N. Prieskorn and J. T. Hupp, *J. Am. Chem. Soc.*, 1993, **115**, 4927.
3. H. N. Ghosh, J. B. Asbury, Y. X. Weng and T. Q. Lian, *J. Phys. Chem. B*, 1998, **102**, 10208.
4. V. H. Smith, *Phys. Scr.*, 1977, **15**, 147.
5. N. Steunou, G. Kickelbick, K. Boubekeur and C. M. Sanchez, *J. Chem. Soc.-Dalton Trans.*, 1999, 3653.
6. J. B. Benedict and P. Coppens, *J. Am. Chem. Soc.*, 2010, **132**, 2938.
7. J. R. Mann, M. K. Gannon, T. C. Fitzgibbons, M. R. Detty and D. F. Watson, *J. Phys. Chem. C*, 2008, **112**, 13057.
8. J. S. Nevins, K. M. Coughlin and D. F. Watson, *ACS Appl. Mater. Interfaces*, 2011, **3**, 4242.
9. M. Gratzel, *Nature*, 2001, **414**, 338.
10. P. Coppens, J. Sokolow, E. Trzop, A. Makal and Y. Chen, *J. Phys. Chem. Lett.*, 2013, 579.
11. A. Makal, J. Benedict, E. Trzop, J. Sokolow, B. Fournier, Y. Chen, J. A. Kalinowski, T. Graber, R. Henning and P. Coppens, *J. Phys. Chem. A*, 2012, **116**, 3359.